Production of Si_3N_4/TiN Nano Composites**

By *Markus Fricke, Ralph Nonninger,* and Helmut Schmidt*

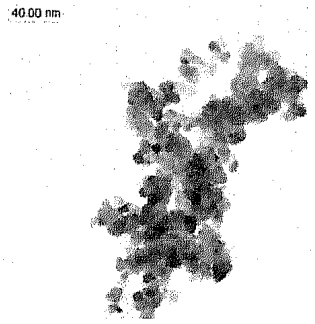

Silicon nitride is used in different applications because of its resistance against thermal shock, high temperature and mechanical load. An appropriate second phase like TiN could make Si_3N_4 attractive for additional applications. This work deals with the introduction of a TiN phase from a nanosize TiN powder into the Si_3N_4 matrix by a single-step wet chemical process.

1. Introduction

Silicon nitride has asserted as a ceramic material for different applications in car manufacturing and the energy industry and as a cutting tool because of its resistance against thermal shock, high temperature and mechanical load.[1,2] In the area of cutting tool applications, requirements for Si_3N_4 ceramics increase with the acceleration of manufacturing processes by means of higher speed and the need for longer standing times.[3] Furthermore, the application field of steel processing has not yet been developed for Si_3N_4 because of its lacking of chemical resistance.[4] But the application range of Si_3N_4 may be enlarged specifically by incorperation of a second phase.

Besides fibers and whiskers, particular additives have also been proven to be useful as a means for the reinforcement of ceramics. Particular reinforcement phases of ZrO_2 or TiC in the μm range in an Al_2O_3 matrix have just enabled the application of Al_2O_3 as a cutting material by enhancement of properties such as toughness or thermal shock resistance.[4] In the last few years the use of nano-sized particles in a ceramic matrix gains interest, because significant enhancement of mechanical properties could be achieved, e.g. by new toughening mechanisms. Different authors[5–7] could verify the increase of strength through use of nanodisperse SiC in an Al_2O_3 matrix by a change of the breaking mode. High temperature properties have been improved by Sternitzke and other authors[8–10] by nanosized SiC particles in a Si_3N_4 matrix. However, so far SiC was only used as a whisker-like reinforcement in cutting materials because of its poor chemical resistance towards Fe-containing materials. On the other hand, TiN serves as an enhancing phase in a Si_3N_4 matrix due to its fundamental properties that are required for the material reinforcement. It is chemically stable against the matrix and shows moderate differences regarding thermal expansion, which could result in residual thermal stress and therefore improves the toughness.[11,12] At the same time, the chemical resistance towards steel is higher than that of Si_3N_4, so that the application range of the cutting tool from ceramic materials could be enlarged.[13] The foundation for the improvement of properties is an optimized manufacturing process considering the enhancement phase.

The use of wet chemical processing routes for the manufacturing of Si_3N_4 composites with commercial sub-μm and μm TiN powders (particle sizes from 0.3 to 10 μm) has already been investigated by different authors.[11,14–16] A two step homogenization and grinding process in alcoholic solvents is used for preparation of this ceramic composite. The sintering additives Al_2O_3 and Y_2O_3 with a total amount of up to 10 wt.-% are homogenized with the initial Si_3N_4 powder during the first step. After drying the dispersion of the TiN powder takes place in a second grinding process step. Compression occurs by hot pressing or gas pressure sintering. Referring to Hermann[14] and Bellosi,[15] coarse TiN particles cause an increase of toughness from 7 up to 10 MPa $m^{0.5}$ and a decrease of strength from 900 down to 600 MPa in case of TiN contents up to 40 vol.-%. The decrease of strength is described by an increase of the defect size caused by TiN ag-

[*] *Dr. M. Fricke, Dr. R. Nonninger, Prof. H. Schmidt*
Institut für Neue Materialien
Saarbrücken (Germany)
E-mail: non@inm-gmbh.de

[**] *This work was promoted by the Bundesministerium for education and investigation (BMBF) inside of the Eureka-project 03 N 500 4B and was executed in cooperation with Dr. R. Meisel (H. C. Starck, Laufenburg) and Dr. G. Brandt (Sandvik Coromant, Stockholm).*

glomerates with particle sizes between 50 and 150 μm.[11] In case of fine TiN particles (<3 μm), prepared by controlled sedimentation of the TiN powders, Bellosi[15] notices an increase of strength from 900 (Si_3N_4) up to 1050 MPa and of toughness from 5 up to 8 MPa $m^{0.5}$ in contrast to Herrmann.[14] While Bellosi attributes the reason for the improvement of the mechanical properties to micro cracking, Herrmann proves crack deflection mechanisms especially at coarser TiN particles (>1 μm).

This work deals with the introduction of a TiN phase from a nanosize TiN powder into the Si_3N_4 matrix by a single-step wet chemical process. The adjustment of the powder surfaces by surface modifiers should enable the preparation of an aqueous multi component suspension containing low contents of the sintering additives MgO and Y_2O_3 in a homogenous distribution. A sintered material of this type has already been proven to be a good cutting material[3,17] and serves as reference. For comparison a Si_3N_4/TiN composite will be prepared by using a nanosized TiN powder from H.C. Starck which is implemented into the preparation process by appropriate surface modification. A comparison of these materials enables us to discuss the influence of TiN on the mechanical properties and microstructure.

2. Experimental

Beside the commercial Si_3N_4 powder (Ube, E10) the sintering additives Y_2O_3 (Starck, grade fine) and MgO (Fluka, schwer) with 1 wt.-% were used. As the second phase nanoscaled TiN-powder (Starck) with a volume fraction of 5 % was useed.

For homogenization of the Si_3N_4-reference the water based $Si_3N_4/MgO/Y_2O_3$ suspension was milled by an attritor with mill balls of Si_3N_4, sieved and finally freeze-dried. The nanoscale TiN surface was modified to produce a homogeneous dispersion of TiN in the water based $Si_3N_4/MgO/Y_2O_3$ slip-system. For the surface modification the washed TiN powder was heated 5 h in ethanol with acetic anhydride under reflux and then sieved and dried. The modified TiN powder was dispersed in the $Si_3N_4/Y_2O_3/MgO$ slip-system and also attritor milled, sieved and freeze dried. The densification of the dried composite-powders was obtained by hot pressing at 1800 °C and 25 MPa for 30 min under N_2 atmosphere in a press of the Thermo Technology company type HP50-7010.

To analyze the materials Si_3N_4, Y_2O_3, MgO, and also the nanoscale TiN-powder with respect to particle size and morphology a scanning electron microscopy (HSEM) of the JEOL-company (type JSM 6400 F) and a transmission electron microscopy (HTEM) of the Phillips company (type CN 200, FEG) were used. The phase content of these powders were analyzed by a X-ray diffraction (XRD) apparatus of the Siemens company (D 500). The specific surface area of the powders was determined by the Brunauer–Emmett–Teller (BET) method. For oxygen- and carbon analysis measuring equipment of the Leco company (RC412 and TC436) were used, while the potentiometric Cl-measurement was realized with a Cl-ionic sensitive electrode. Data of the flow behavior and viscosity of the suspensions were taken from the rotary viscosimeters (Physica Typ Rheolab MC20). For data of zeta potential of various powders, a zeta potentiometer (Malvern) was used. Microstructural characterization of the densified samples was performed by HSEM on the polished and plasma etched surfaces and HTEM in combination with energy dispersive X-ray (EDX) analysis. For density measurements the Archimedean method was used. The α/β-phase content was analyzed by the method of Garrera and Messier.[18]

The Young's modulus (E) was measured on the hot pressed samples by the frequency resonance method. The fracture toughness (K_{1C}) was evaluated by the direct crack measurement method with the load of 98 N in a hardness tester Leco using the formula proposed by Niihara et al.[19] On the same apparatus the Vickers hardness (HV) has been measured on the polished surfaces with a load of 98 N. The flexual strength was measured on the polished samples 3 mm × 4 mm × 25 mm in a four-point bending fixture (Zwick type1446).

3. Results and Discussion

3.1. Powder Characterization and Suspension Preparation

The morphology of the powders used for the preparation of the reference ceramic in the state of delivery is shown in Figure 1 by HREM. The results of the powder characterization are gathered up in Table 1.

The Si_3N_4 material shows spherical particles with particle sizes of about 500 nm. In addition there are some whisker-like particles. The phase distance of the powder is made of 98 % α-Si_3N_4, which should allow a coarsening microstructure with elongated β-grains during densification that improve fracture toughness.[20] The particles of the used Y_2O_3 powder are plate-like with an average size of 700 nm. The particle surface of 15.5 m^2/g, which is higher than that of the Si_3N_4 powder (10.5 m^2/g), is a result of this kind of particle shape, because the plate-like particles have a larger surface in relation to their volume compared with spherical particles. The MgO powder also shows a plate-like morphology with average particle sizes of 300 nm with a particle surface of 34.4 m^2/g.

Table 1. Characterization of the properties of the used powders.

	Si_3N_4	Y_2O_3	MgO	n-TiN
phase content	98% α-Si_3N_4 2 % β-Si_3N_4	crystaline	Periclase partial amorph	Osbornite
BET [m^2/g]	10.5	15.5	34.4	40.4
C-Content [%]	0.02	0.19	1.10	0.01
O-Content [%]	1.25	–	–	0.59
Cl-Content [%]	–	–	–	1.10

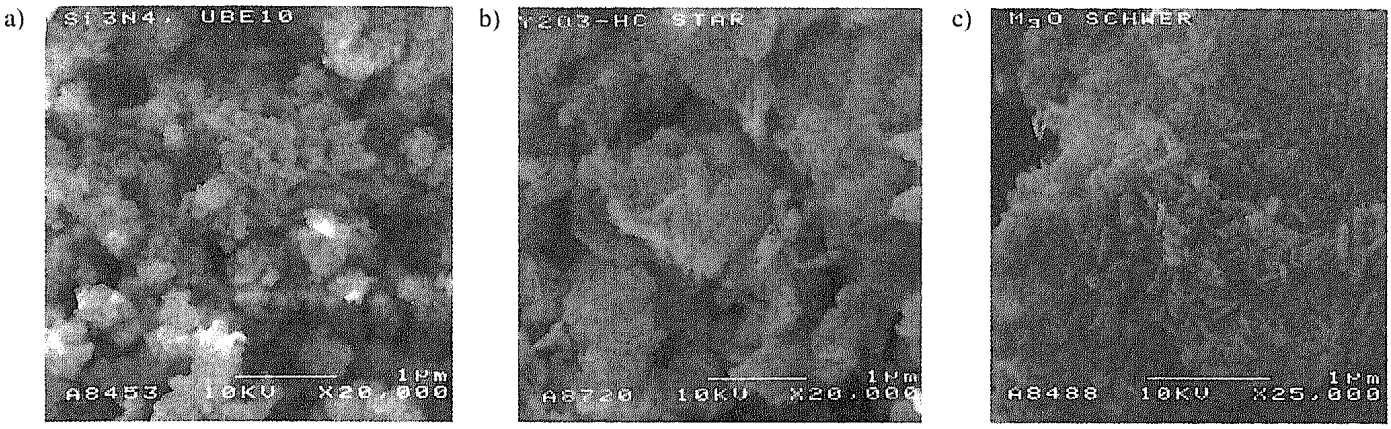

Fig. 1. HSEM pictures of the used powders: a) Si_3N_4, b) Y_2O_3, and c) MgO.

Zeta-potential measurements have been carried out for the determination of the surface properties of the powders. The zeta potential curves listed in Figure 2 look similar for all three initial powders with an isoelectric point at pH-values of 5.1 (Y_2O_3), 6.1 (Si_3N_4), and 6.4 (MgO). Therefore, an electrostatic stabilization of the aqueous multi-component suspension should be possible at both an acidic and base pH-range. Nevertheless the dissolution of the additive powders MgO and Y_2O_3 in the acidic pH range is known[21] and leads to destabilization of the multi-component suspension because of the increased ionic quantity and decreased surface charge of the powder particles. For that reason the processing of the multi-component suspension was realized in the base pH-range.

Figure 3 show the flow behavior of the $Si_3N_4/Y_2O_3/MgO$-suspension at pH 10 for various solid contents. It can be seen that the suspensions with solid contents up to 32 vol.-% (60 wt.-%) develop a newtonian flow behavior with viscositys below 10 MPa s. This rheological behavior proves the electrostatic stabilization of the various powder particles. With solid contents of 37 vol.-% (65 wt.-%) a Bingham flow is obtained, which may be related to the formation of a network structure of weakly bonded particle aggregates with increasing particle-particle interaction.[22]

To produce a Si_3N_4 reference ceramic the $Si_3N_4/MgO/Y_2O_3$ slipsystem with a solid content of 60 wt.-% was attritor-milled, freeze-dried and finally hot pressed.

In comparison to the Si_3N_4 reference a Si_3N_4 ceramic composite is farbricated with a second phase of TiN by the use of a nanoscale powder. The HTEM investigation of these powder in Figure 4 shows spherical primary particles with a average size between 10 and 20 nm. The properties in Table 1 show a high powder surface of 40 m^2/g and a Cl content of 1.10 %, which makes it necessary to wash the powder for the further arrangement. The Cl content could complicate the stabilization of the multi component suspension in a base pH range, because of the pH shift of the multi component suspension during dispersion of the powder.

For deagglomeration of the nanosize TiN-powder in a aqueous suspension a surface modification with a succinic acetoanhydride was done. The effect of the surface modifier on the surface properties explains the results of the zeta potential measurement shown in Figure 5. The isoelectric point changee from pH4.2 to pH3.1 for the modified powder. The zeta potential curve of the modified powder shows a plateau from a pH-value of 5 up to the base pH range, which can be attributed to the deprotonation of the surface groups. Figure 6 shows a model for the reaction of the modifier with the

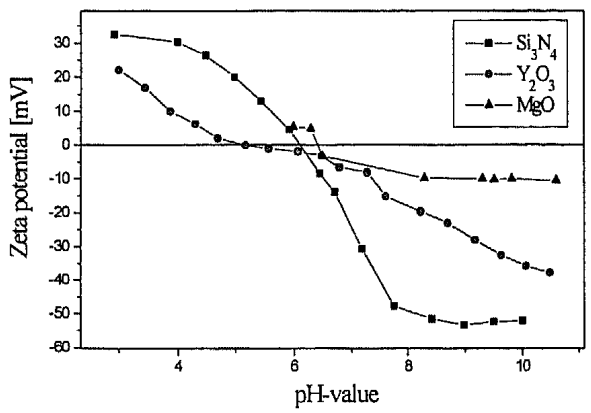

Fig. 2. Zeta potential measurement of the used powders titrated from a pH range 10 to (tetramethylammoniumhydroxid) 3 with HCl for Si_3N_4 and Y_2O_3 and acetic acid for MgO.

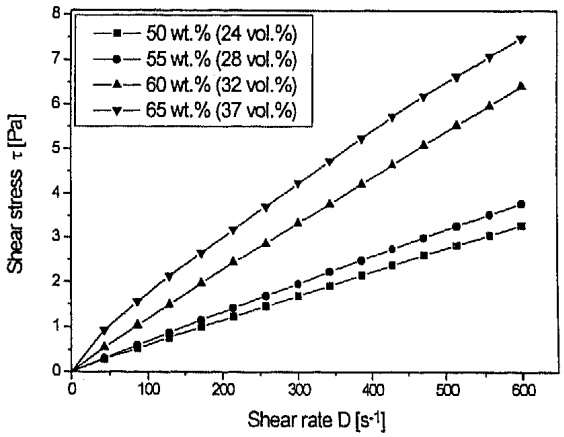

Fig. 3. Flow behavior of the $Si_3N_4/Y_2O_3/MgO$-suspension for various solid contents at a pH-value of 10.

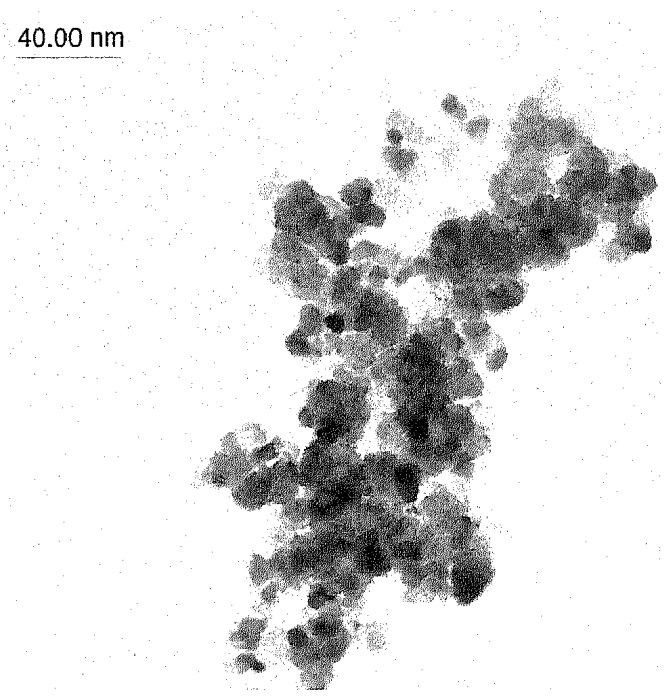

Fig. 4. HTEM-picture of the nanosize TiN-powder.

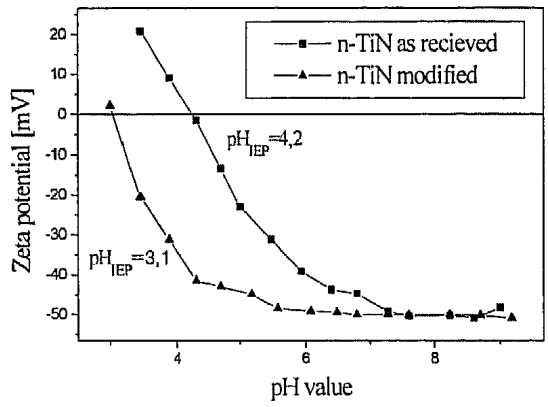

Fig. 5. Zeta potential measurement of the nanosize TiN powder as recieved and with surface modification with a succinicacidanhydridesilane titrated from pH 10 (tetramethylammoniumhydroxid) to pH 3 (HCl).

oxydic TiN powder surface and the hydrolyzation of the anhydride in water. The change of the isoelectric point can be connected with the formation of carboxy groups of the hydrolyzed anhydride ring.

Better stabilization of the surface modified TiN-powders in aqueous medium in base pH range can be shown in Figure 7 on the basis of rheological properties of concentrated suspensions. In contrast to the unmodified powders the TiN-suspensions with a surface powder treatment show, for solid contents of up to 40 wt.-%, newtonian flow behavior and prove the stabilization of an uncoagulated colloidal system. The stabilization of the modified powder particles in the aqueous system may be caused by steric repulsive mechanismen beside the electrostatic forces of the negative charged carboxyl groups (Fig. 6).

The same process as used for the fabrication of the Si_3N_4 reference ceramic, was used for the produciton of a composite powder with TiN 5 vol.-%. The rheological characterization of the milled multi-component suspensions with a solid content of 60 wt.% shows in Figure 8 a newtonian flow behavior for both systems with viscosities of 6.3 (Si_3N_4/MgO/Y_2O_3/TiN) respective 4.8 mPa s (Si_3N_4/MgO/Y_2O_3). A comparison of the rheological behavior of the Si_3N_4/MgO/Y_2O_3-suspension (60 wt.-%) with the results in figure 3 shows the decreasing viscosity (10 to 5 mPa s) because of the attritor milling process.

Due to the surface modification of the TiN-powder the addition of the nanosize powder in an aqueous Si_3N_4/Y_2O_3/MgO slipsystem was sucessful. The freeze dried composite powders were in comparison to the Si_3N_4 reference hot pressed at 1800 °C and 25 MPa for 30 min under N_2 atmosphere and reach densities of 3.27 g/cm^3 for the composite with a TiN volume fraction of 5 % (3.20 g/cm^3 for the Si_3N_4 reference). These results agree with densities >99 % of the theoretical value for both ceramic materials (Table 2).

3.2. Microstructural Characterization and Mechanical Properties

The investigation of the microstructure of the various materials was conducted by HREM on polished, plasma etched samples. In Figure 9 microstructures of the composite containing 5 vol.-% of nanosize TiN are shown in comparison to the Si_3N_4 reference material. The elongated Si_3N_4 are visible in this illustration as is the regular structure of the glass phase at the grain boundaries. It is obvious from the analysis that the microstructure of the Si_3N_4 matrix system did not change by addition of the nanosize TiN. The TiN particles in sample (b) have a homogenously distributed grain size of 0.1–1 μm and are placed at the boundaries of the Si_3N_4 particles. On the

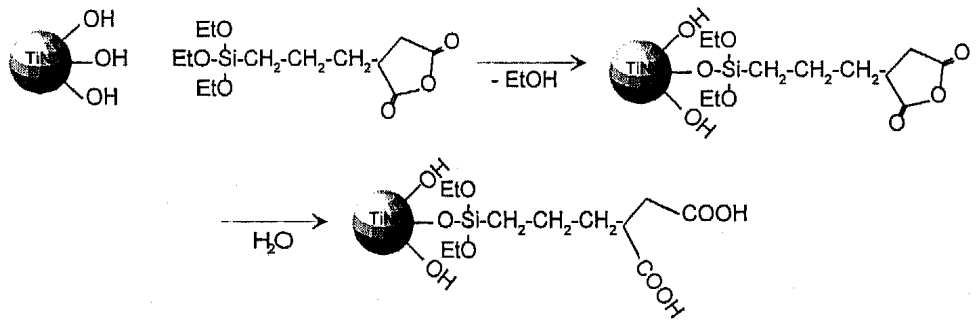

Fig. 6. Model for the reaction of the (3-triethoxysilylpropyl)succinic acetic anhydride silane with the oxidized TiN-powder surface.

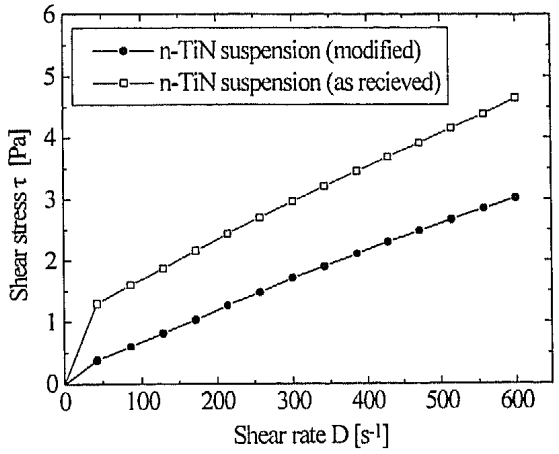

Fig. 7. Comparison of the flow behavior of TiN suspensions with 40 wt.-% solid content.

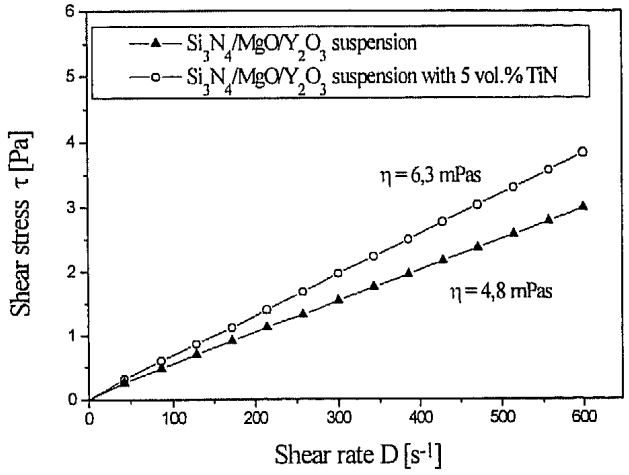

Fig. 8. Flow behavior of the multi component slipsystems after attritor milling with solid content of 60 wt.-%.

other hand some TiN particles with a size of about 100 nm are placed within the particles. In spite of the homogenous distribution of the TiN particles it must be considered that the size of the TiN particles in the composite sample (b) is not equivalent to the particle size of the nanosize TiN powder of 10–20 nm. Since the TiN phase is, according to Herrmann,[14] involved in the liquid phase formation at the early sintering state because of the TiO_2 on its surface, these TiN particles are able to grow by solution and reprecipitation processes. The TiN particles positioned at the Si_3N_4 grain boundaries get pushed together by the coarsening of the matrix structure during the ongoing sintering process and sinter because of the densification temperature of 1800 °C, which is much higher than the sintering temperature of nanosize TiN.[23,24]

The addition of TiN has an influence on the phase content of the Si_3N_4 matrix material because of the TiO_2 on the powder surface, as is shown in Table 2. Since according to Herrmann[14] the TiO_2 is transformed into TiN by formation of SiO_2 according to Equation 1, there is a higher liquid phase content created during the densification, which results in an acceleration of the α/β-phase transformation under equivalent sintering conditions. Thus, the material with TiN contains a β-content of 82 %, while the Si_3N_4 reference ceramic only contains 75 %.

Table 2. Comparison of the mechanical properties between the Si_3N_4-reference ceramic and the Si_3N_4/TiN composite (5 vol.-%).

density [g/cm³]	Si_3N_4	Si_3N_4/TiN (5 vol.-%)
	3.20 (99.9%)	3.27 (99.1%)
β-phase content [%]	75	82
Young's Modul [GPa]	324.2	326.1
hardness HV_{10} [GPa]	18.5	17.8
K_{IC} [MPa*m$^{0.5}$]	6.2/6.9	6.4/7.2
strength [MPa]	953 ± 69	1006 ± 119

These results are verified by HTEM analysis of the Si_3N_4/Si_3N_4 and Si_3N_4/TiN grain boundaries, shown in Figure 10. In this analysis the glass phase at the grain boundaries both between Si_3N_4 particles and between Si_3N_4 and TiN particles becomes visible with a thickness of about 1 nm. The EDX analysis of the grain boundary phase reveals a composition of the elements Si, O, Y, and Mg. Since there is no Ti found in this phase, it can be concluded that the described transformation of TiO_2 to TiN under formation of SiO_2 out of Si_3N_4 is correct.

$$3\,TiO_2 + Si_3N_4 \longrightarrow 3\,SiO_2 + 3\,TiN + 0.5\,N_2 \qquad (1)$$

The effects of the TiN phase on the mechanical properties of the Si_3N_4 ceramic were investigated on composite samples with a TiN content of 5 vol.-% in comparison with a Si_3N_4 reference material. The results are presented in Table 2. The mechanical properties of the materials show only slight differences concerning the E-modul. On the other hand the hardness of the material without TiN phase is higher. This is caused by a higher α-phase content,[25] because this phase has a higher hardness in comparison to the β-phase. The toughness grows slightly when TiN is added, which is caused by the higher β-phase content that enables the formation of the elongated microstructure. The declaration of two different toughness values takes the texture effect of the elongated structure into account, which is caused by uniaxial hot pressing. The Si_3N_4/TiN composite material has a strength of about 1000 MPa, which is higher than that of the Si_3N_4 reference material. This can be attributed to the increased fracture toughness. Al in all, differences in the mechanical properties caused by the use of TiN are small. The improvement of the fracture toughness of up to 3 MPa m$^{0.5}$ shown by Herrmann and Bellosi[14,15] could not be verified, but TiN contents of up to 40 wt.-% with TiN grain sizes of >1 μm were used by them.

4. Conclusion

This examination shows that the preparation of a homogenous Si_3N_4/TiN composite material with TiN grain sizes of 0.1–1 μm by adjustment of the powder surfaces by preparation of a aqueous multi-component suspension is possible. The structure analysis shows that the TiN particles, mainly

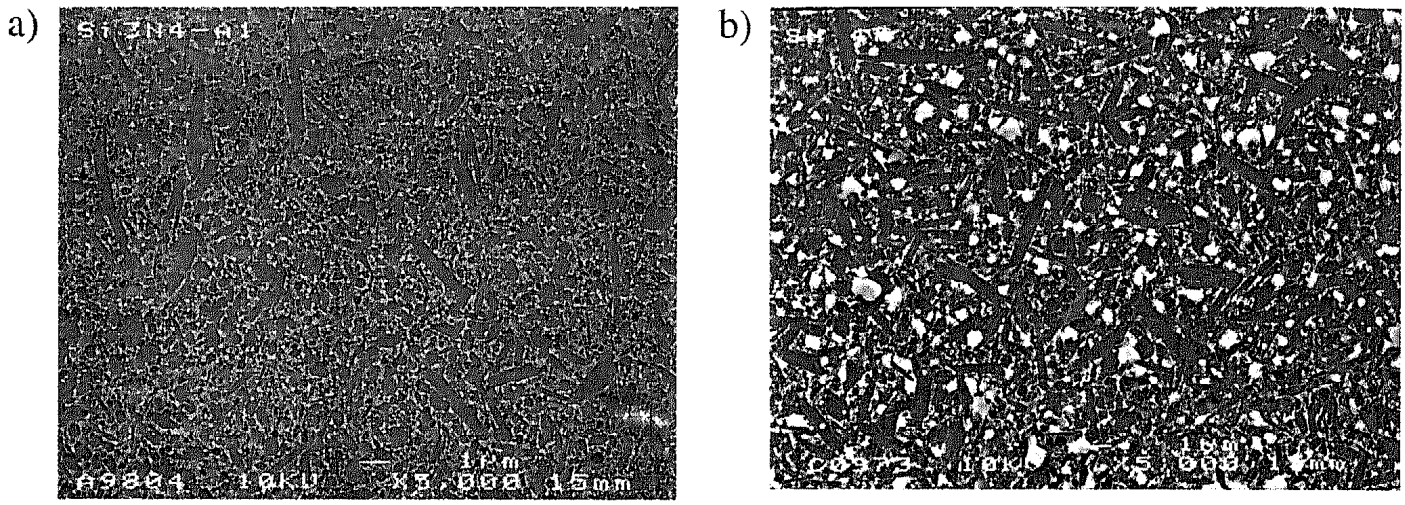

Fig. 9. HREM pictures of polished and plasma etched Si_3N_4 reference ceramic (a) and the Si_3N_4 composite with 5 vol.-% TiN (b).

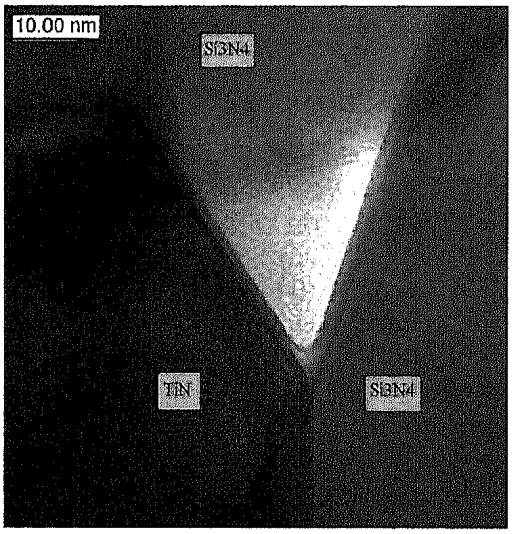

Fig. 10. HTEM-picture of the grain boundary phase between Si_3N_4–Si_3N_4 and Si_3N_4–TiN grains (Si_3N_4 composite with 5 vol.-% TiN).

positioned at the grain boundaries, have grown because of the densification process. Because of the transformation of TiO_2 on the surface there is an increase of the β-phase content in the composite, which has a stronger influence on the material properties than the TiN at the grain boundaries. For a complete analysis of the effects of nanosize TiN powders in a Si_3N_4 matrix experiments with varying sintering conditions and TiN contents are still to be made. Since a content of 5 vol.-% does not show a fundamental improvement of the mechanical properties, it is necessary to check the development of these properties with higher TiN contents.

[1] J. G. Heinrich, H. Krüner, *Ber. Dtsch. Keram. Ges.* **1995**, *72*, 167.

[2] R. N. Katz, *Ind. Ceram.* **1997**, *17*, 158.

[3] A. Krell, in *Pulvermetallurgie in Wissenschaft und Praxis* (Ed: R. Ruthard), Frankfurt **1997**, pp. 57–75.

[4] G. Brandt, *Ceramic technology international* **1995**, pp. 77–80.

[5] K. Niihara, *J. Ceram. Soc. Jpn.* **1991**, *99*, 945.

[6] M. Sternitzke, B. Derby, R. J. Brook, *J. Am. Ceram. Soc.* **1998**, *81*, 41.

[7] L. C. Stearns, J. Zhao, M. P. Harmer, *J. Eur. Ceram. Soc.* **1992**, *10*, 473.

[8] M. Sternizke, *J. Eur. Ceram. Soc.* **1997**, *10*, 1061.

[9] A. Rendtel, H. Hübner, M. Hermann, C. Schubert, *J. Am. Ceram. Soc.* **1998**, *81*, 1095.

[10] A. Rendtel, H. Hübner, M. Hermann, C. Schubert, *J. Am. Ceram. Soc.* **1998**, *81*, 1109.

[11] Y. G. Gogotsi, *J. Mater. Sci.* **1994**, *29*, 2541.

[12] T. Nagaoka, K. Hirao, S. Kanzaki, *J. Ceram. Soc. Jpn.* **1992**, *100*, 612.

[13] S. Casto, E. Valvo, E. Lucchini, *Key Eng. Mater.* **1996**, *114*, 105.

[14] M. Hermann, C. Schubert, W. Hermel E. Meißner, G. Ziegler, *Ber. Dtsch. Keram. Ges.* **1996**, *73*, 434.

[15] A. Bellosi, S. Guicciardi, A. Tampieri, *J. Eur. Ceram. Soc.* **1992**, *9*, 83.

[16] S. N. Shina, T. N. Tiegs, *Ceram. Eng. Sci. Proc.* **1995**, *16*, 489.

[17] R. D. Nixon, P. K. Mehrotra, *Ceram. Eng. Sci. Proc.* **1997**, *18*, 211.

[18] C. Gazzara, D. Messier, *Ceram. Bull.* **1977**, *56*, 777.

[19] D. Munz, T. Fett, in *Mechanisches Verhalten keramischer Werkstoffe*, Springer, Berlin **1989**, pp. 37–41.

[20] G. Wötting, G. Ziegler, *Sprechsaal* **1987**, *120*, 96.

[21] L. Frassek, G. Wötting, in *Pulvermetallurgie in Wissenschaft und Praxis*, VDI-Verlag, Düsseldorf **1991**, *7*, 403.

[22] A. Nagel, G. Petzow, *J. Eur. Ceram. Soc.* **1989**, *5*, 371.

[23] T. Rabe, R. Wäsche, *Nanostruct. Mater.* **1995**, *6*, 357.

[24] T. Yamada, M. Shimada, M. Koizumi, *Ceram. Bull.* **1980**, *59*, 611.

[25] H. Miao, L. Qi, G Cui, *Key. Eng. Mater.* **1996**, *114*, 135.